ENC-2022-0700

INVESTIGATION OF THE BIOENERGETIC POTENTIAL OF SOYBEAN HUSKS FOR USE IN THERMOCHEMICAL PROCESSES BY PHYSICOCHEMICAL AND MORPHOLOGICAL ANALYSIS

Julie Brenda Santos da Silva
Federal Institute of Maranhão, Post-graduate Program in Mechanical Engineering, Department of Mechanics and Materials, Avenida Getúlio Vargas, 04, Monte Castelo, São Luís (MA).
julie_brenda@hotmail.com

Jefferson Rodrigues Ferreira
Federal University of Maranhão, Department of Mechanical Engineering, Processes and Thermal Systems Laboratory, Avenida dos Portugueses, 1966, Bacanga, São Luís (MA).
jefferson.rodrigues@discente.ufma.br

Glauber Cruz
Federal University of Maranhão, Department of Mechanical Engineering, Processes and Thermal Systems Laboratory, Avenida dos Portugueses, 1966, Bacanga, São Luís (MA).
cruz.glauber@ufma.br

Abstract. *Due to the growing energy demand and damaging consequences of using fossil fuels in the energy matrix, several studies investigate new and promising renewable energy sources. Among these sources, biomass has devoted scientists' attention due to its versatility, availability, cost, and effect considered neutral for greenhouse gas emissions. In this context, this study presents a physicochemical and morphological evaluation of soybean husks for bioenergy production through thermochemical conversion processes. For examination of biomasses, X-Ray Diffraction (XRD), Fourier Transform Infrared (FTIR), Ultimate Analysis (UA), and Scanning Electronic Microscopy (SEM) analyzes were performed. For the XRD analysis, selected biomass presented a Crystalline Index (CI) of 38.41%. The sample revealed some functional groups such as alcohols, alkanes, alkenes, acids, amides, aromatics, and alkyl halides employing FTIR analysis. The ultimate analysis exhibited the amounts of carbon (41.81±0.92%), hydrogen (5.39±0.16%), nitrogen (1.00±0.09%), and oxygen (51.80±0.00%). The SEM images revealed the morphology and texture of soybean husks, which appear amorphous, disorganized, and porous, also showing structures that indicate the presence of hemicellulose, cellulose, lignin, protein, and other compounds. The studied biomass presented compositional, vibrational, structural, and morphological characteristics similar to other biomasses already used for bioenergy generation, demonstrating the excellent potential for thermochemical conversion, especially for direct combustion processes.*

Keywords: *amorphous, combustion, crystallinity, energy, waste.*

1. INTRODUCTION

The harmful consequences of fossil fuels excessive use are massive to be non-discussed (Olatunji *et al*., 2020). Due to the consumption of fossil fuels being the main human activity to cause the greenhouse gases emissions (CO_2, CH_4, N_2O), non-gases products, and particulates (aerosols and black carbon); scientists, environmentalists, politicians, and other parts of civil society agree that is urgent to shift from the fossil energy source to environmentally friendly and carbon neutral energy sources (Daneshvar *et al*., 2022). In 2020, International Energy Agency (IEA, 2022) registered a decrease of about 2 billion tons of CO_2, this contraction can be related to the Covid-19 pandemic. However, the return to "business as usual" push the energy production and industrials processes to the highest CO_2 emissions levels recorded of 36.3 gigatons (Gt) in 2021, this value is 6% higher than the previous year (2020), which is evidenced the need in adopting new strategies for carbon reduction (IEA, 2022).

Because of the hurry to diversify the energy matrix, biomass has gained much attention in past decades (Ashraf *et al.*, 2021). Bioenergy, mainly, produced by biomass supplied around 90% of industrial demand in 2019 and represented one-tenth of the total primary energy source using renewables sources in 2021 (IEA, 2022; REN21, 2022).

Brazil is often recognized as one of the biggest bioenergy producers in the world, occupying the second position of world investor in ethanol and biodiesel production in 2022, and the second position in biopower capacity in the same year (REN21, 2022). Brazil presents 48.3% of its internal energy stock composed of renewable sources, *i.e.*, 12.6% is derived from hydraulic, 8.9% from firewood and charcoal, 19.1% from sugarcane waste, and 7.7% from another source (EPE, 2021). Thus, the world energy commercialization is expected to increase, and to supply this request, is crucial to investigate, improve, and expand the range of the lignocellulosic biomasses available (Alves *et al.*, 2022).

Lignocellulosic biomass is a renewable, abundant, costless, and versatile feedstock for bioenergy production. However, is necessary to overcome the occurrence of some provision problems caused by seasonality, harvest, and quantity of specific biomass (Alves *et al.*, 2022). Consequently, the investigation of new feedstocks with potential bioenergy to feed thermochemical devices became important and has been gaining recognition in recent years (Cruz *et al.*, 2020).

Agribusiness is a sector that generates a large amount of waste and it is a great opportunity for the production of lignocellulosic feedstocks (Rodionova *et al.*, 2017). Brazil presents notorious agriculture and is the biggest soybean producer in the world, with 37% of the production share in 2021, resulting in 135 million tons of soybean (EMBRAPA, 2021; IBGE, 2022).

In this context, the *commodities* generate a large amount of waste, which represents a new potential lignocellulosic biomass for thermochemical conversion systems, for this reason, this study presents the evaluation of Brazilian biomass for use in thermochemical processes, *e.g.*, soybean husks, which represent one of the biggest sources of lignocellulosic feedstock. For this biomass performed Ultimate Analysis (UA), X-Ray Diffraction (XRD), Fourier Transform Infrared (FTIR), and Scanning Electronic Microscopy (SEM images), for investigating their structural, vibrational, compositional, and morphological characteristics.

2. MATERIALS AND METHODS

This section presents the main steps and experimental settings for the Brazilian biomass characterization for use in thermochemical processes, following the methodology developed by Cruz (2015) as can be observed in the 2.1 to 2.5 sections.

2.1 Sample origin and preparation

The soybean husks were obtained from a soybean producer farm, located in the Balsas (MA) city (latitude: -7,53292; longitude: -46,035). In the preparation step, the samples were washed in running water for the impurity's removal and dried on a stove (*Tecnal TE-393/80L*) at 60 °C for 48 h for moisture removal. After this process, the samples were grounded in knife and forage mills (*Tecnal TE-648* and *Trapp TRF 400 Super*, respectively) for particle size reduction, and sieved for an average granulometry of ≈ 328 µm (ASTM series, 45 and 50 meshes).

2.2 Ultimate Analysis (UA)

The ultimate analysis was performed to discover the biomasses' chemical composition, and it was possible to obtain the contents of carbon (C), oxygen (O), hydrogen (H), nitrogen (N), and sulfur (S) of the samples, using an Elementary Analyzer (*Perkin Elmer, 2400 CHNS-O*). The oxygen percentage was calculated by a difference of 100%.

2.3 X-Ray Diffraction (XRD)

The sample's crystallographic structures were evaluated by mean of X-Ray diffractometer (XRD) (*Bruker D8 advance*), which employed the CuKα radiation ($\lambda = 1.541$ Å, 40 kV - 40 mA). The diffraction angle (2θ) ranged from 5 to 70° and the sweep speed of 0.05° s^{-1}.

The crystalline index (CI) was calculated using Segal's method, which is represented in Eq. (1), where I_{002} denotes crystalline region diffraction and I_{am} indicates the amorphous region diffraction intensity, which for the CuKα radiation the 2θ value is around of 22.5° and 18.0° for these intensities, respectively (Xu *et al.*, 2013).

$$CI_\% = \frac{(I_{002} - I_{am})}{I_{002}} \cdot 100 \qquad (1)$$

2.4 Fourier Transform Infrared (FTIR)

The Fourier Transform Infrared (FTIR) was used to identify the main structural components employing the vibrational characteristics of the biomasses. The measurements were performed in a spectrophotometer (*Shimadzu IR-Prestige-21*) from 4000 to 400 cm^{-1}, and the samples were prepared with KBr (potassium bromide).

2.5 Scanning Electronic Microscopy (SEM)

The morphological and textural structures of Brazilian harvest waste were observed by Scanning Electronic Microscopy (SEM) (*Leo Electron Microscopy LEO440*). The experiment was performed in a vacuum and the samples were submitted to a gold bath (metallization).

3. RESULTS AND DISCUSSION

Results showed characteristics of these biomasses, which are related to the potential use of these biomasses as lignocellulosic feedstock for thermochemical conversion systems, for this reason, such results are discussed and presented in sections 3.1 to 3.5.

3.1 Ultimate Analysis (UA)

The average values of C, H, N, and S contents for the soybean husks are presented in Fig.1. A remarkable result is the absence of sulfur (S), maybe the ultimate analysis performed was not capable to detect this element. The average carbon, hydrogen, and nitrogen contents of this study are lower by 1.8; 17.2, and 37.0%, respectively, related to the values for the soybean hulls of Indian origin (C = 42.3%; H = 6.4% and N = 1.7%) found by Rastrogi, Jha, and Sarma (2016). The soybean hulls studied by these authors also not presented significant sulfur contents, which revealed that soybean hulls, as well as the biomass used in this research, are not prone to the formation of SO$_X$, or can tend to produce amounts of these gases at insignificant levels (Rastrogi *et al.*, 2016).
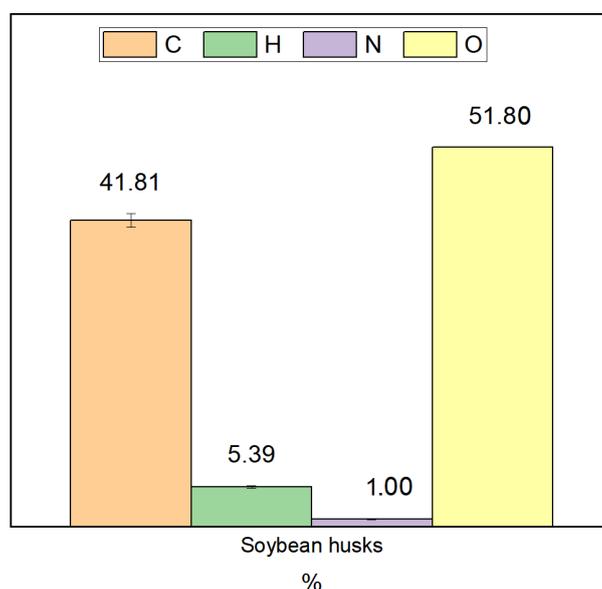

Figure 1. Histogram representation of Ultimate Analysis data for the soybean husks.

The soybean sample presented low nitrogen and sulfur contents, these elements directly cause the formation of NO$_X$ and SO$_X$ emissions, one of the main substances promoting air pollution and generating respiratory diseases. Such emissions also increase the solar reflection coefficient by changing the global temperature. In thermochemical conversion systems, these gases are associated with corrosion problems in ovens, boilers, ducts, etc (Bilsback *et al.*, 2019; Sahoo *et al.*, 2020). Therefore, soybean husks as raw material are less likely to form pollutants and consequently, a small contribution to the formation of greenhouse gases, as well as proper functioning the prevention and/or reduction of system corrosion

Hydrogen and oxygen contents are related to the propensity to generate water steam (H$_2$O)$_v$ and carbon dioxide (CO$_2$) during thermochemical conversion systems. The significant amount of carbon in biomass designates the presence of fixed carbon that represents a good conversion efficiency because this component releases a greater amount of energy per unit of mass, as well as favors charcoal gasification processes (Miranda *et al.*, 2020). The high carbon

amount and low hydrogen content revealed a low possibility of excessive moisture production and the presence of carbonaceous components rich in profitable energies (Miranda *et al.*, 2020).

3.2 X-Ray Diffraction (XRD)

The X-Ray Diffraction is plotted in Fig. 2. The I_{am} is located at $2\theta = 18.23°$ and I_{002} at $2\theta = 22.28°$, and the crystalline index (CI) resultant is 38.41%. The results for the CI of the soybean samples showed values higher in 34.9% than those soybean hulls collected in the State of Rio Grande do Sul (Brazil), which presented a CI value of 25.0%, using the same calculation method for measuring this parameter (Rambo *et al.*, 2015). Another interesting characteristic is the presence of a peak at $2\theta = 35°$, which is related to the [101] lattice, corresponding to a cubic crystal, probably characterized by the presence of silicon (Si) or quartz crystals (Rocky & Thompson, 2020).
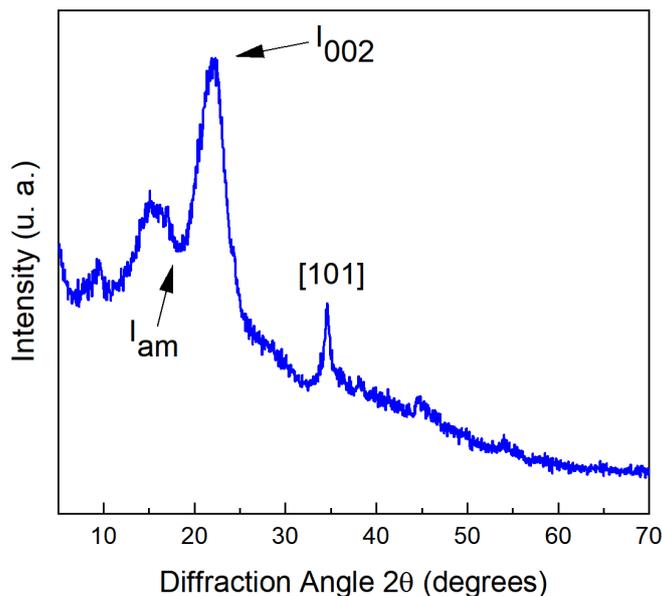

Figure 2. X-Ray diffractogram of the soybean husks for structural analysis and crystalline index calculation.

The crystalline region of biomass is associated with the presence of cellulose, while the amorphous region relates to the presence of lignin and hemicellulose (Wang *et al.*, 2017).

The sample of this study is considerably amorphous, and consequently, it presents lower thermal stability, being highly favourable for use in direct combustion processes or systems, because the high reactivity assists in the preservation of the burning flame, but for coal production, a high amount of volatiles present in biomass is harmful, generating a thermal degradation of these substances at low temperatures (Martinez *et al.*, 2019). However, even though the soybean husks presented amorphous structures, it was not possible to conclude that this biomass is not profitable for thermal processes, *e.g.*, pyrolysis and gasification (Bora *et al.*, 2021).

3.3 Fourier Transform Infrared (FTIR)

The Fourier Transform Infrared resulting curve in transmittance mode is shown in Fig. 3. Figure 3 also reveals the main functional groups identified for the soybean husk samples and the respective peaks associated with each group that is located in the FTIR spectra.

The hydroxyl group identified at 3335 cm^{-1} is related to the presence of moisture in organic materials, even though soybean husks have passed through the drying process, this biomass still presents residual or intrinsic moisture and, also, can characterize the presence of alcohols and/or phenols (Huang *et al.*, 2020).

The bands identified as C-H and -C-H located at 2916 and 1375 cm^{-1}, respectively, are related to the presence of CH_2 and CH_3 branches in hydrocarbon chains, which are attributed to the presence of lipids and esters, and triglycerides, respectively (Manjunatha & Girisha, 2021).

The C=C bonds (1419 cm^{-1}) are related to the presence of aromatic compounds, which are the main constituents of lignin (Wang *et al.*, 2017). The C-O linkage is called the alcohol group, which is a molecular fragment that may be related to alcohols (1150-1050 cm^{-1}) and acids (1320-1210 cm^{-1}) (*e.g.*, fatty, acetic, formic acids, etc) present in extracts found in vegetables, as well as by the presence of hemicellulose and lignin in biomass. For the soybean husks sample, this referred group was identified at 1249 cm^{-1} (Kumneadklang *et al.*, 2019; Rawal *et al.*, 2018; Wang *et al.*, 2017).

Alkanes and haloalkanes can be detected by groups =C-H (702 cm^{-1}), C-Cl (665 cm^{-1}), and C-Br (594 cm^{-1}), which are attributed to organic compounds and halogens found in different biomasses, for instance, sorghum and corn (Kotaiah Naik *et al.*, 2017).
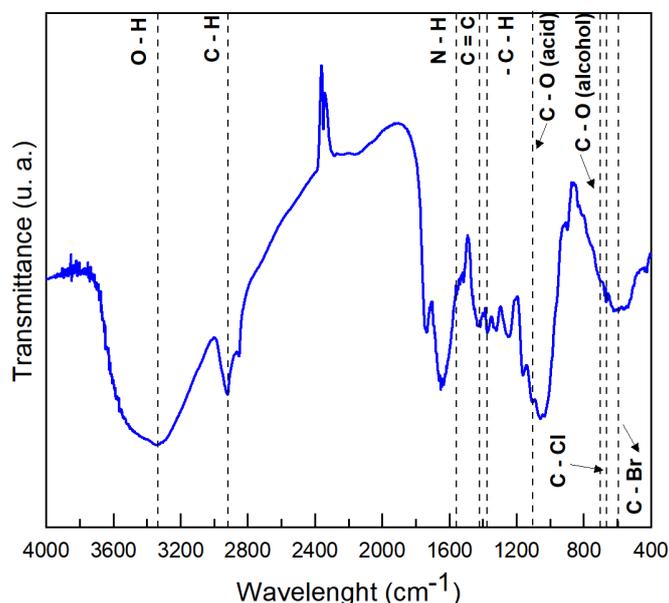

Figure 3. Fourier Transform Infrared spectra for the soybean husks in transmittance mode.

It is possible to note that the biomass studied presented a high concentration of organic and inorganic compounds, some of these compounds indicating strong connections like those that occur between carbon-carbon and that present high bonding energy from 346-835 kJ mol^{-1} to 273 K, which indicate the need of a high energy content to be broken, because of such elements present high thermal stability, and others linkages between carbon-chlorine (327 kJ mol^{-1} at 273 K) and carbon-bromine (285 kJ mol^{-1} at 273 K), probably due to the presence of haloalkanes, respectively (Brown *et al.*, 2021).

3.4 Scanning Electronic Microscopy (SEM images)

The images of the Scanning Electronic Microscopy (SEM) are revealed in Fig. 4. The micrographs of soybean husks presented in Figures 4 (a-c) revealed their morphological and textural structures, and are consistent with the results of the crystalline index (XRD) because these samples are amorphous structures, irregular and fragmented, the later, possibly, due to the grinding process.
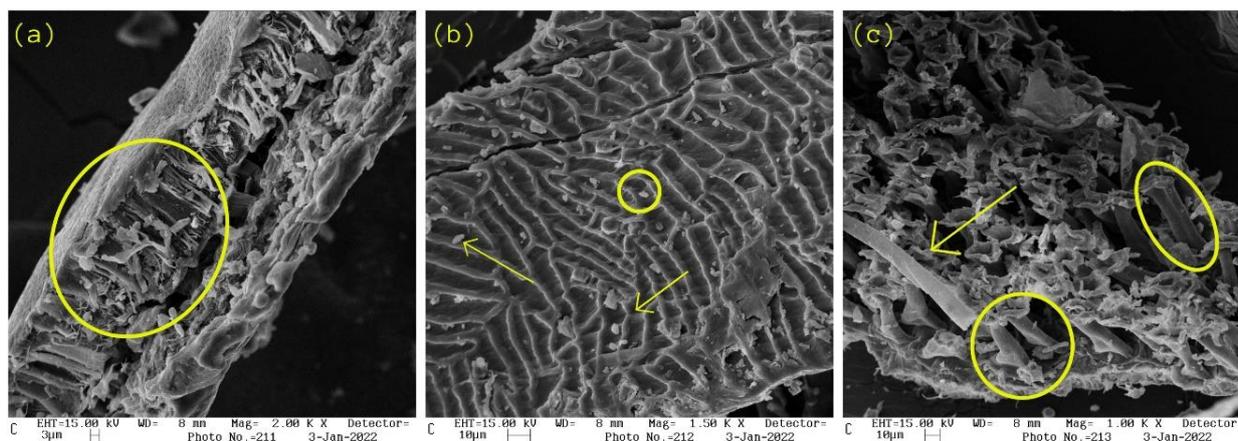

Figure 4. Scanning Electronic Microscope (SEM) images of the soybean husks: (a) 2000x, (b) 1500x, and (c) 1000x magnification.

The structure presented in Fig. 4a resembles the cross-section of the isolated soybean protein film developed by Zhou *et al.* (2021). Using it, was possible to state that structure presented in this figure is a typical example of the basic topography of a soybean protein along with other structures that this presents.

Figure 4b also reveals a structure similar to the soybean protein, as well as on its entire surface presents possible fragmented crystals, which can be represented by the light grey or white spots, clearly showing the presence of silica in this biomass (Da Cunha-Pereira *et al*., 2020; Zheng *et al*., 2014).

The stem-shaped structures presented in Fig. 4c are similar to cellulose nanofibers of sugarcane bagasse, possibly these also are soybean cellulose filaments dispersed in the samples (Prakash Menon *et al*., 2017).

Figures 4(a-c) are consistent with the results obtained by Cunha-Pereira *et al*. (2020), as well as the biomass of this study presented many intercellular spaces (above 10 μm), with a strong influence on the modes of intermolecular heat transfer in biomass, interfering in the integral thermal properties of this due to the diffusivity and thermal conductivity, that are distinct in the longitudinal and lateral directions of the plant cells (Basu, 2010).

4. CONCLUSION

In this study was obtained the compositional, structural, vibrational, morphological, and textural characteristics of the soybean husks for application in thermoconversion processes.

Soybean husks presented a carbon-rich composition, which represents the presence of great carbon bonds that can release a considerable amount of energy during thermochemical processes. The low crystalline index and amorphous regions revealed a reactive feedstock, which is promising for direct combustion systems. Soybean husks presented functional groups, with high-energy linkage bonds that are profitable for charcoal production under pyrolysis processes.

In this sense, soybean husks are an excellent alternative for bioenergy generation, not only by the amount of waste available, but also due to their versatile energetic characteristics, which can be destined to different thermochemical processes (combustion, pyrolysis, oxyfuel combustion, and gasification).

5. ACKNOWLEDGEMENTS

6. REFERENCES

Alves, J. L. F., da Silva, J. C. G., Mumbach, G. D., de Sena, R. F., Machado, R. A. F., & Marangoni, C. (2022). Prospection of cattle coconut (Syagrus cearensis) as a new bioenergy feedstock: Insights from physicochemical characterization, pyrolysis kinetics, and thermodynamics parameters. *Renewable Energy*, *181*, 207–218. https://doi.org/10.1016/j.renene.2021.09.053

Ashraf, M., Ramzan, N., Khan, R. U., & Durrani, A. K. (2021). Analysis of mixed cattle manure: Kinetics and thermodynamic comparison of pyrolysis and combustion processes. *Case Studies in Thermal Engineering*, *26*(May), 101078. https://doi.org/10.1016/j.csite.2021.101078

Basu, P. (2010). Biomass Characteristics. In *Biomass Gasification Design Handbook* (First Edit). © 2010 Elsevier Inc. https://doi.org/10.1016/b978-0-12-374988-8.00002-7

Bilsback, K. R., Kerry, D., Croft, B., Ford, B., Jathar, S. H., Carter, E., Martin, R. V., & Pierce, J. R. (2019). Beyond SOxreductions from shipping: Assessing the impact of NOx and carbonaceous-particle controls on human health and climate. *Environmental Research Letters*, *15*(12). https://doi.org/10.1088/1748-9326/abc718

Bora, J., Deka, P., Bhuyan, P., Sarma, K. P., & Hoque, R. R. (2021). Morphology and mineralogy of ambient particulate matter over mid-Brahmaputra Valley: application of SEM–EDX, XRD, and FTIR techniques. *SN Applied Sciences*, *3*(1), 1–15. https://doi.org/10.1007/s42452-020-04117-8

Brown, LeMay, Busten, Murphy, & Woodward. (2021). *8.1 Strength of Covalent Bonds*. Chemistry Libretexts. https://chem.libretexts.org/@go/page/25291

Cruz, G., Silva, A. V. S., Da Silva, J. B. S., Nazaré Caldeiras, R., & Souza, M. E. P. (2020). Biofuels from oilseed fruits using different thermochemical processes: opportunities and challenges. *Biofuels, Bioproducts and Biorefining*, *14*(3), 696–719. https://doi.org/10.1002/bbb.2089

Cruz, G. (2015). *Características Físico-Químicas De Biomassas Lignocelulósicas E a Correlação Entre Suas Emissões E Os Resíduos Gerados Sob Diferentes Condições Atmosféricas Em Um Forno Tubular De Queda Livre (Dtf)*.

Da Cunha-Pereira, F., Matte, C. R., Costa, T. M. H., Dupont, J., Antônio, M., & Ayub, Z. (2020). Treatment and characterization of biomass of soybean and rice hulls using ionic liquids for the liberation of fermentable sugars. *An Acad Bras Cienc*, *92*(3), 20191258. https://doi.org/10.1590/0001-3765202020191258

Daneshvar, E., Wicker, R. J., Show, P. L., & Bhatnagar, A. (2022). Biologically-mediated carbon capture and utilization by microalgae towards sustainable CO_2 biofixation and biomass valorization – A review. *Chemical Engineering Journal*, *427*(June 2021), 130884. https://doi.org/10.1016/j.cej.2021.130884

EMBRAPA. (2021). *Dados econômicos - Portal Embrapa*. Embrapa.Br. https://www.embrapa.br/soja/cultivos/soja1/dados-economicos

EPE, B. (2021). *Relatório Síntese Balanço Energético Nacional Relatório Síntese*. https://www.epe.gov.br/sites-pt/publicacoes-dados-abertos/publicacoes/

Huang, H., Liu, J., Liu, H., Evrendilek, F., & Buyukada, M. (2020). Pyrolysis of water hyacinth biomass parts: Bioenergy, gas emissions, and by-products using TG-FTIR and Py-GC/MS analyses. *Energy Conversion and Management*, *207*(March), 112552. https://doi.org/10.1016/j.enconman.2020.112552

IBGE. (2022). *Tabela 7832: Área plantada, área colhida, produção e rendimento médio, por ano da safra e produto das lavouras*. Sidra. https://sidra.ibge.gov.br/tabela/7832#resultado

IEA. (2022, March). *Global Energy Review: CO2 Emissions in 2021 – Analysis - IEA*. https://www.iea.org/reports/global-energy-review-co2-emissions-in-2021-2

Kumneadklang, S., O-Thong, S., & Larpkiattaworn, S. (2019). Characterization of cellulose fibers isolated from oil palm frond biomass. *Materials Today: Proceedings*, *17*, 1995–2001. https://doi.org/10.1016/j.matpr.2019.06.247

Manjunatha, S. S., & Girisha, S. T. (2021). Characterization of microalgal biomass through Fourier transforms infrared (FT-IR) spectroscopy. *International Journal of Botany Studies*, *6*(1), 57–60.

Martinez, C. L. M., Alves Rocha, E. P., Oliveira Carneiro, A. de C., Borges Gomes, F. J., Ribas Batalha, L. A., Vakkilainen, E., & Cardoso, M. (2019). Characterization of residual biomasses from the coffee production chain and assessment of the potential for energy purposes. *Biomass and Bioenergy*, *120*(November 2018), 68–76. https://doi.org/10.1016/j.biombioe.2018.11.003

Miranda, M. R. da S., Veras, C. A. G., & Ghesti, G. F. (2020). Charcoal production from waste pequi seeds for heat and power generation. *Waste Management*, *103*, 177–186. https://doi.org/10.1016/j.wasman.2019.12.025

Olatunji, O. O., Akinlabi, S., Madushele, N., Adedeji, P. A., & Ndolomingo, M. J. (2020). Geospatial investigation of physicochemical properties and thermodynamic parameters of biomass residue for energy generation. *Biomass Conversion and Biorefinery*. https://doi.org/10.1007/s13399-020-00723-z

Prakash Menon, M., Selvakumar, R., Suresh Kumar, P., & Ramakrishna, S. (2017). Extraction and modification of cellulose nanofibers derived from biomass for environmental application. *RSC Advances*, *7*(68), 42750–42773. https://doi.org/10.1039/C7RA06713E

Rambo, M. K. D., Schmidt, F. L., & Ferreira, M. M. C. (2015). Analysis of the lignocellulosic components of biomass residues for biorefinery opportunities. *Talanta*, *144*, 696–703. https://doi.org/10.1016/j.talanta.2015.06.045

Rastrogi, A., Jha, M. K., & Sarma, A. K. (2016). A comparative study of kinetics for combustion versus pyrolysis of Mesua ferrea husk, soya husk, and Jatropha curcas husk using thermogravimetry and different methods. *Energy Sources, Part A: Recovery, Utilization and Environmental Effects*, *38*(10), 1355–1363. https://doi.org/10.1080/15567036.2014.913094

Rawal, S., Joshi, B., & Kumar, Y. (2018). Synthesis and characterization of activated carbon from the biomass of Saccharum bengalense for electrochemical supercapacitors. *Journal of Energy Storage*, *20*(July), 418–426. https://doi.org/10.1016/j.est.2018.10.009

Ren21. (2022). *RENEWABLES 2021 GLOBAL STATUS REPORT*. https://www.ren21.net/wp-content/uploads/2019/05/GSR2021_Full_Report.pdf

Rocky, B. P., & Thompson, A. J. (2020). Characterization of the crystallographic properties of bamboo plants, and natural and viscose fibers by X-ray diffraction method. *Journal of the Textile Institute*, *0*(0), 1–9. https://doi.org/10.1080/00405000.2020.1813407

Rodionova, M. V., Poudyal, R. S., Tiwari, I., Voloshin, R. A., Zharmukhamedov, S. K., Nam, H. G., Zayadan, B. K., Bruce, B. D., Hou, H. J. M., & Allakhverdiev, S. I. (2017). Biofuel production: Challenges and opportunities. *International Journal of Hydrogen Energy*, *42*(12), 8450–8461. https://doi.org/10.1016/j.ijhydene.2016.11.125

Sahoo, A., Kumar, S., & Mohanty, K. (2020). A comprehensive characterization of non-edible lignocellulosic biomass to elucidate their biofuel production potential. *Biomass Conversion and Biorefinery*. https://doi.org/10.1007/s13399-020-00924-6

Wang, S., Dai, G., Yang, H., & Luo, Z. (2017). Lignocellulosic biomass pyrolysis mechanism : A state-of-the-art review. *Progress in Energy and Combustion Science*, *62*, 33–86. https://doi.org/10.1016/j.pecs.2017.05.004

Xu, F., Shi, Y. C., & Wang, D. (2013). X-ray scattering studies of lignocellulosic biomass: A review. *Carbohydrate Polymers*, *94*(2), 904–917. https://doi.org/10.1016/j.carbpol.2013.02.008

Zheng, A., Zhao, Z., Chang, S., Huang, Z., Wu, H., Wang, X., He, F., & Li, H. (2014). Effect of crystal size of ZSM-5 on the aromatic yield and selectivity from catalytic fast pyrolysis of biomass. *Journal of Molecular Catalysis A: Chemical*, *383–384*(April 2018), 23–30. https://doi.org/10.1016/j.molcata.2013.11.005

Zhou, X., Dai, Q., Huang, X., & Qin, Z. (2021). Preparation and characterizations of antibacterial-antioxidant film from soy protein isolate incorporated with mangosteen peel extract. *E-Polymers*, *21*(1), 575–589. https://doi.org/10.1515/epoly-2021-0058

7. RESPONSIBILITY NOTICE

The authors are the only ones responsible for the printed material included in this paper.